

Theory and practice of simulation of optical tweezers

Ann A. M. Bui, Alexander B. Stilgoe, Isaac C. D. Lenton, Lachlan J. Gibson, Anatolii V. Kashchuk, Shu Zhang, Halina Rubinsztein-Dunlop, Timo A. Nieminen

The University of Queensland, School of Mathematics and Physics, Brisbane QLD 4072, Australia

Journal of Quantitative Spectroscopy and Radiative Transfer **195**, 66-75 (2017)

Abstract

Computational modelling has made many useful contributions to the field of optical tweezers. One aspect in which it can be applied is the simulation of the dynamics of particles in optical tweezers. This can be useful for systems with many degrees of freedom, and for the simulation of experiments. While modelling of the optical force is a prerequisite for simulation of the motion of particles in optical traps, non-optical forces must also be included; the most important are usually Brownian motion and viscous drag. We discuss some applications and examples of such simulations. We review the theory and practical principles of simulation of optical tweezers, including the choice of method of calculation of optical force, numerical solution of the equations of motion of the particle, and finish with a discussion of a range of open problems.

Keywords: Optical tweezers, laser trapping, optical force, optical torque, light scattering

PACS: 42.25.Fx, 42.50.Wk, 42.50.Tx, 87.80.Cc

1. Introduction

The optical forces in optical tweezers result from the interaction of the trapping beam with the trapped particle. Thus, the computation of optical forces and torques is a light scattering problem. While this is a challenging problem, and much work remains to be done, there has been a great deal of progress, and for many situations, it is straightforward to obtain the optical force and torque. However, if we wish to simulate the behaviour of particles within optical tweezers, the optical force is only one of the necessary ingredients. We will discuss some applications and examples of such simulations, and review the theory and principles of simulation of optical tweezers.

1.1. The need for simulations

Since it is usually straightforward to calculate the optical force on a trapped particle, it is possible to characterise the trap by determining the force as a function of particle position (and orientation if the particle is non-spherical). At first glance, this appears to provide complete information about the trap, and we might ask what need there is to perform simulations. There are two main answers to this question. First, it is not always feasible to generate such a force map of the trap. Second, while a force map of this type does contain complete information about the trap in some sense, it doesn't directly answer all questions we might have about the trap. In particular, the dynamics of a particle in the trap depend on its interaction with the surrounding environment as well as the optical force. The dominant elements of that interaction are often Brownian motion and viscous drag, but other types of interaction can

also be important. Where the dynamics themselves are the object of study (e.g., escape probabilities, synchronised dynamics of trapped particles, etc.) or have a major impact on the behaviour of interest (e.g., in the simulation of measurements to test calibration procedures), it is necessary to take these non-optical into account.

The first of these cases results from situations with many degrees of freedom. To map the force as a function of position with useful (but not high) resolution typically requires about 30 steps along each degree of freedom (giving about 10 steps as forces change from zero to a maximum value). If it takes 1 second to calculate the optical force at a single position, this will give required computational times for different degrees of freedom (DOF) of:

- 1 DOF** Example: calculating axial and/or radial force-position curves; finding equilibrium position along beam axis, and axial and radial spring constants. 30 to 60 points. Time: 0.5–1 minute.
- 2 DOF** Example: mapping force for a spherical particle in a rotationally symmetric trap (e.g., circularly polarised Gaussian beam). $30^2 \approx 1000$ points. Time: ≈ 15 minutes.
- 3 DOF** Example: mapping force for a spherical particle in a trap lacking rotational symmetry (e.g., linearly polarised Gaussian beam). $30^3 \approx 30,000$ points. Time: ≈ 8 hours.
- 4 DOF** Example: mapping force for a rotationally symmetric non-spherical particle in a rotationally symmetric trap. $30^4 \approx 10^6$ points. Time: ≈ 10 days.
- 5 DOF** Example: mapping force for a rotationally symmetric non-spherical particle in a trap lacking rota-

Email address: timo@physics.uq.edu.au (Timo A. Nieminen)

tional symmetry; two spherical particles in a rotationally symmetry trap. $30^5 \approx 3 \times 10^7$ points. Time: ≈ 1 year.

6 DOF Example: mapping force for a non-spherical particle lacking rotational symmetry in a trap lacking rotational symmetry; two spherical particles in a trap lacking rotational symmetry. $30^6 \approx 10^9$ points. Time: ≈ 30 years.

Additional particles will add 2–3 translational degrees of freedom (depending on the symmetry of the trap) and 0, 2, or 3 rotational degrees of freedom (depending on the symmetry of the particle). If the trapping beam varies in time, this adds another degree of freedom, although if the time variation consists of switching between a small number of fixed positions, this will only multiply the number of required calculations and the computational time by a small number.

The above times do not take parallelisation of the calculations into account—this can readily bring one or two more degrees of freedom into feasibility. However, even with parallelisation, we will still rapidly run into the limits of practicality due to the exponential growth of computational time with the number of degrees of freedom. Therefore, it can be necessary to resort to simulation to obtain information we might prefer to find from a complete force map. This will typically involve non-spherical particles or multiple particles.

On the other hand, even if it is feasible to calculate a complete force map for the trap, we might still wish to perform simulations. In particular, a force map doesn't contain information about the dynamics of a particle in the trap. While the optical force—which the force map provides—is a key factor in the dynamics of the particle, the particle is also influenced by other forces: viscous drag, thermal forces (driving Brownian motion), and possibly interaction with other parts of the environment. If the dynamics are of interest, we can use simulation to uncover it.

To explore the dynamics of a particle in the trap, it can be possible, and advantageous, to use a pre-calculated force map. If it is feasible to calculate a complete force map with reasonable resolution, the optical force at any position can be found by interpolating between the points in the force map where the forces are known. This interpolation can be performed very quickly (the computational implementation should avoid copying the force map to perform the interpolation). The required accuracy of the interpolated force will determine the minimum resolution of the force map. This resolution of the force map, along with the required spatial extent of the simulation, determines the number of points required in the force map. If this exceed the number of time steps required in the simulation, then direct calculation will be more efficient. However, often the number of time steps will be much greater, and using a force map to find the optical force will be much more efficient. This will often be the case for optical traps with 2 or 3 degrees of freedom. An extreme case of this is where the particle remains very close to its equilibrium position, and the trap can be represented in terms of a spring constant (which will generally

be a diagonal tensor, with different spring constants in different directions, or even a non-diagonal tensor).

1.2. Applications of simulations

There are many possible applications of this. Most fall into three broad categories: simulations to understand experiments that have been performed, simulations to predict the results of potential experiments, and simulations to explore optical traps and the dynamics of trapped particles in ways that are not accessible experimentally.

The first of these, simulations of experiments that have been performed, can be simply seeing if a simulated experiment matches measured results. This can be very useful if the experimental results are surprising. If agreement between simulated and measured results is obtained, the physics and models used in the simulation adequately model reality. If agreement is not obtained, then the model is either incomplete (e.g., physics not included significantly affect the measured results) or elements of the model are incorrect (invalid approximations, mathematical errors, incorrect implementation in software, numerical errors).

For example, Stilgoe et al. (2011) observed the appearance of a third trapping equilibrium position as two optical traps were moved close together. In this case, simulations were valuable for confirming that the third trap can be produced in this two-beam configuration, even if the two trapping beams are not mutually coherent, i.e., the third trap doesn't depend on interference between the two trapping beams.

Haghshenas-Jaryani et al. (2014) used a combination of experiment and simulation to explore the transition from overdamped motion to underdamped motion as the size of trapped particles was reduced.

Volpe et al. (2014) observed the trajectories of particles in a laser speckle pattern, and compared the observed trajectories with simulated trajectories in speckle patterns with the same average intensity. In this case, the simulations do not aim to exactly replicate the experimental situation, but to replicate it in a statistical sense. That is, the speckle fields in the simulations have the same statistical properties as the experimental speckle fields. Qualitative and statistical agreement between observed and simulated trajectories demonstrates that the observed behaviour is general, and does not arise due to some abnormality in the experimental case.

Wu et al. (2009) determined the non-conservative force field from the motion of a trapped particles. Their experimental results were supported by simulations. In the experiment, the force field is inferred from the motion of the particle, while in the simulations, the force field is known. This allows validation of the procedure used to obtain the experimental force field.

Similarly, the knowledge of the optical forces available in simulations was used to validate escape force calibrations on chromosomes by Khatibzadeh et al. (2014). Measurements of the force required to pull chromosomes free from an optical trap were performed in order to estimate the forces exerted on chromosomes by a cell during cell division (mitosis) from the power required to halt the motion (Ferraro-Gideon et al., 2014). Since the exact size and

refractive index of the chromosomes were uncertain, a further series of experiments and simulations on the escape of spheres from optical traps due an applied force were performed (Bui et al., 2015), revealing the dependence of the escape trajectory, and the escape force, on the trapping power and rate of increase of the applied force.

Simulations that deliberately differ from the experiments can show the effect of the difference on observations or measurements. For example, Czerwinski et al. (2009) used Allan variance to quantify noise in optical tweezers setups. Simulations were used to obtain (simulated) data free of noise and long-term drift, providing a suitable baseline for comparison with experimental results.

As noted above, simulations are often necessary when the system has many degrees of freedom, such as when there are non-spherical or multiple particles. Brzobohatý et al. (2015b) used simulations to explore the shape dependence of the trapping behaviour of non-spherical gold nanoparticles. Brzobohatý et al. (2015a) used simulations to support experiments rotational dynamics of multiple spheroidal particles in a dual beam trap. Following observations of optically-driven oscillations of ellipsoidal particles (Mihiretie et al., 2014), Loudet et al. (2014) performed simulations to understand the physical basis of the observed behaviour.

In these examples above, simulations were performed to support experiments. The opposite of this, where experiments are performed to support simulations, is also common. The aim of the simulations can vary greatly, from demonstration of the feasibility of a particular experiment before performing it, to using simulation as a tool to help design the experiment, through to a broad series of exploration via simulation with experiments being performed to validate the simulations. In this last case, the experimental work might consist of only a small fraction of the range covered by the simulations. If the simulation method and implementation is already known to be reliable from previous validation, then the reported work might consist purely of simulations.

Some of this more simulation-focussed work is similar to the experiment-focussed work described above. For example, similar to the work of Wu et al. (2009), Pesce et al. (2009) also explored the non-conservative forces in optical traps.

As noted above, simulations allow the optical forces to be known, and are therefore valuable for testing calibration methods. Simulated measurements, of the type that would be measured experimentally in order to calibrate an optical trap, or to determine the optical force field from the motion of a trapped particle, can be generated, and the same analysis that would be performed on experimental data can be performed on the simulated data. The simulated calibration or force measurement can be compared with the actual optical force in the simulation. Examples of simulations of this type include Volpe et al. (2007), Volpe and Petrov (2006), and Gong et al. (2006). Such simulations can also readily include non-spherical particles (Bui et al., 2013). Similar comparison on known quantities in the simulation and simulated measurement of these quantities can be carried out for methods to measure prop-

erties of the surrounding medium, such as its viscoelasticity (Fischer and Berg-Sørensen, 2007).

An application where the trapping beam varies in time is the simulation of control methods, where the position or power of the beam can be varied to achieve a desired effect (Banerjee et al., 2012; Aguilar-Ibañez et al., 2011; Li et al., 2013). Variation of the beam power over time introduces an additional degree of freedom, and movement of the beam introduces 2 to 4 additional degrees of freedom (time and 1 to 3 spatial degrees of freedom). Similarly, improved trapping methods can be explored (Taylor et al., 2015).

Simulations can be aimed at a more general exploration of the behaviour of optically-trapped particles. These can be specifically investigating the dynamics of trapped particles (Banerjee et al., 2009; Xu et al., 2005; Deng et al., 2007; Ren et al., 2010; Cao et al., 2016; Trojek et al., 2012). Another common goal is the study of the behaviour of non-spherical particles, where the additional degrees of freedom motivate the use of simulations (Simpson and Hanna, 2010a,b; Cao et al., 2012). These can include optically-driven micromachines. One example is the use of simulations to determine the optimum illumination to drive a corrugated rotor with maximum torque efficiency, while retaining stable three-dimensional trapping (Loke et al., 2014). Another example is an optical "wing", consisting of a semi-cylindrical rod (Artusio-Glimpse et al., 2013; Simpson et al., 2012). Such a structure can generate lift—an optical force acting normal to the direction of illumination—in addition to the expected radiation pressure force. Simulations by Artusio-Glimpse et al. (2014) show that complex rocking motion can occur. The simulations allow the effects of time-varying illumination, producing a parametrically driven nonlinear bistable oscillator, to be explored.

Finally, simulations can be useful for educational purposes (Volpe and Volpe, 2013; Perkins et al., 2010)

For some of these simulations, it is not necessary to accurately model the dynamics of the particle. For example, to determine the equilibrium position and orientation of a non-spherical particle within the trap, it is not necessary to correctly model the viscous drag. The translational and rotational drag tensors can be approximated by Stokes drag for a sphere, even if the particle is non-spherical. Brownian motion can be ignored, although it (or random jitter providing similar random motion) can be useful for preventing the particle from getting stuck in an unstable equilibrium. This can happen, for example, if the particle is a flat disc, which would tend to align with its symmetry axis normal to the beam axis (Bayouduh et al., 2003), but will be in an unstable equilibrium if the simulation is begun with the disc on the beam axis, with its symmetry axis along the beam axis.

However, for many types of simulations, where actual or prospective experiments are being simulated, it is often important to accurately model the dynamics, and to include all important details of the interaction of the particle with its environment. At minimum, this can be expected to include viscous drag and Brownian motion.

2. A recipe for simulation, part 1

The motion of a particle of mass m subject to a force $\mathbf{F}(t)$ can be calculated from

$$m \frac{d^2 \mathbf{r}}{dt^2} = \mathbf{F}(t), \quad (1)$$

given initial conditions for the position $\mathbf{r}(t=0)$ and velocity $\mathbf{v}(t=0)$. The force $\mathbf{F}(t)$ is the sum of contributions from various sources:

$$\begin{aligned} \mathbf{F}(t) = & \mathbf{F}_{\text{optical}} + \mathbf{F}_{\text{weight}} + \mathbf{F}_{\text{buoyancy}} \\ & + \mathbf{F}_{\text{drag}} + \mathbf{F}_{\text{Brownian}} + \mathbf{F}_{\text{other}}, \end{aligned} \quad (2)$$

where we have explicitly listed the optical force, weight, buoyancy, viscous drag, and thermal forces driving Brownian motion. We have also included $\mathbf{F}_{\text{other}}$ to represent any other forces present. The weight and buoyancy are straightforward, with

$$\mathbf{F}_{\text{weight}} = m\mathbf{g} = \rho_{\text{particle}} V \mathbf{g} \quad (3)$$

and

$$\mathbf{F}_{\text{buoyancy}} = \rho_{\text{medium}} V \mathbf{g}, \quad (4)$$

where V is the volume of the particle, ρ_{particle} and ρ_{medium} are the densities of the particle and the surrounding medium, and \mathbf{g} is the local gravitational acceleration. These can almost always be treated as constant, and present no difficulty for numerical solution of the differential equation (1).

The optical force $\mathbf{F}_{\text{optical}}$ is the force that typically has the most attention paid to it in discussion of optical tweezers and optical trapping. Depending on the particle in question (and the optical trap), calculation of the optical force can vary from a formidable computational challenge to an already-solved problem with freely-available implementations. We will discuss the calculation of optical forces in the following section. For the moment, we will consider the spatial scale over which the optical force varies, since this directly affects the solutions of differential equation (1). In a typical optical trap, the energy density varies from small to large values over a distance of half a wavelength or more. As a result, the optical forces will vary from small to large over a similar length scale, or over a distance comparable to the particle radius. For example, when a large spherical particle is centred on the beam axis in typical Gaussian beam optical tweezers, the force is zero, and when the edge of the particle is on the beam axis, the radial force is approximately maximum. For such a trap, we can assume that the length scale over which the optical force varies is the larger of the two (i.e., the maximum of the half-wavelength and the particle radius). However, even for large particles, the force can vary over the half-wavelength scale, if interference effects are important, such as when trapping in interference fringes produced by mutually-coherent counter-propagating beams. Knowledge of the length scale of variation in the optical force allows us to estimate a suitable maximum distance to allow the particle to move over a time step when numerically solving equation (1).

The viscous drag force has major effects on the numerical solution of the differential equation describing the motion. We will discuss details of the calculation of the viscous drag later, and restrict the current discussion to these effects on the solution. Since, typically, trapped particles are microscopic and are trapped in a viscous environment, the interaction between the particle and the fluid is characterised by very low Reynolds numbers. In this case, the viscous drag is linearly related to the velocity:

$$\mathbf{F}_{\text{drag}} = \mathbf{D}\mathbf{v}, \quad (5)$$

where \mathbf{D} is a 3×3 drag tensor. Commonly, it is simply stated that since the Reynolds number is very low, we can neglect the inertial term in equation (1) (recalling that the Reynolds number is the ratio of inertial effects to viscous effects in fluid motion), reducing equation (1) to

$$0 = \mathbf{F}(t). \quad (6)$$

Substituting (5), we obtain the first-order differential equation

$$\begin{aligned} -\mathbf{D} \frac{d\mathbf{r}}{dt} = & \mathbf{F}_{\text{optical}} + \mathbf{F}_{\text{weight}} + \mathbf{F}_{\text{buoyancy}} \\ & + \mathbf{F}_{\text{Brownian}} + \mathbf{F}_{\text{other}}. \end{aligned} \quad (7)$$

Note that differential equation (7) assumes that the particle is always moving at terminal velocity, with viscous drag balancing the sum of the other forces. When is this condition satisfied? If a particle is initially at rest in a fluid, and a force \mathbf{F} is suddenly turned on, the approach to terminal velocity $\mathbf{v}_0 = -\mathbf{D}^{-1}\mathbf{F}$ will be characterised by a time constant τ such that

$$\mathbf{v}(t) = \mathbf{v}_0(1 - \exp(-t/\tau)). \quad (8)$$

The time constant τ is

$$\tau = m|\mathbf{v}_0|/|\mathbf{F}|, \quad (9)$$

which, for a spherical particle, becomes

$$\tau = 2\rho_{\text{particle}} a^2 / (9\eta), \quad (10)$$

where a is the radius of the particle, and η is the (dynamic) viscosity of the surrounding medium. Notably, this is independent of the force. For a particle of radius $a = 1 \mu\text{m}$ in water, this gives a time constant of $\tau \approx 2.4 \times 10^{-7} \text{s}$. If we are calculating the motion of the particle using a time step Δt large compared to this (e.g., $\Delta t > 10\tau$), we can safely use equation (7). If we are using a time step similar to or smaller than τ , we should, strictly speaking, use equation (1). In practice, if the force only changes by a small amount over the time step Δt , the particle will already be moving at close to terminal velocity, and equation (7) will yield acceptable results. Haghshenas-Jaryani et al. (2014) consider a case where the difference between equations (1) and (7) matters over short times.

Motion at the very low Reynolds numbers typical in optical traps is outside our everyday experience. Purcell (1977) gives an excellent and accessible overview.

Brownian motion presents a serious difficulty: numerical solution of differential equations such as (1) and (7) typically depend on using a time step sufficiently short so that

the time-varying quantities in the equations (the forces, the position, and the velocity) only vary by a small amount over the time step. However, no matter how short a time step is chosen, classical Brownian motion (i.e., Brownian motion in a continuous fluid Einstein (1956)) always varies by a large amount. Therefore, it is simplest to remove Brownian motion from our differential equations, and treat it separately. We will return to this point after discussion of optical forces, viscous forces, and Brownian motion.

The final force in our differential equations, $\mathbf{F}_{\text{other}}$, can represent many possible forces. For example, adhesion forces between particles or particles and the microscope slide, electrostatic forces, magnetic forces, and more. Needless to say, some of these forces can be challenging to model accurately. In some cases, a similar approach to that suggested above for Brownian motion will be useful: remove the force from the differential equation, and treat it separately.

Finally, for non-spherical particles and some spherical particles, it is necessary to consider rotational motion as well as translational motion. In this case, our differential equation will include optical torques, viscous drag torque (which will be linearly related to the angular velocity by a rotational drag tensor), and other torques. These can be treated in a similar manner to their translational counterparts. Rotational Brownian motion can be treated in a similar manner to translational Brownian motion. Weight and buoyancy can often be ignored, since for many particles, they produce no torque about the centre of the particle. One complication is that it is often desirable to perform the calculations of optical force and torque in a coordinate system fixed to the particle, necessitating transformations between the particle frame and the stationary frame. Due to the analogous nature of rotational motion compared with translational motion, the rotational equations of motion can be readily written following the translational equations of motion, replacing masses with moments of inertia, forces with torques, and translational drag tensors with rotational drag tensors. It should be noted that for particles with a chiral shape, rotational and translational motion can be coupled through viscous drag Moffatt (1977); in this case, an addition coupling tensor will be included in both the translational and rotational equations of motion. For descriptions of simulations involving rotational motion, including equations of motion, see Cao et al. (2012); Bui et al. (2013).

3. Optical forces and torques

The computational modeling and simulation of optical tweezers is essentially a light scattering problem (Nieminen et al., 2001, 2014). The trapping beam interacts with the trapped particle—this is the scattering aspect of the problem—and a force results. As there are a large number of computational approaches to light scattering (Kahnert, 2003), there are a large number of computational approaches to calculating optical forces (Nieminen et al., 2014; Jones et al., 2015). A complete review of all of the methods would be a monumental (and book-length, if not multi-volume) task, and we will not attempt it here. Instead, we will discuss the elements of calculation of optical forces

that are most important for deciding which method will be used for such calculations, and refer readers to appropriate technical literature for particular methods.

We will begin with an overview of the T-matrix method and why it is often the method of first choice for simulations. Note that for a spherical particle, the T-matrix method is essentially equivalent to generalised Lorenz–Mie theory (GLMT) (Gouesbet, 2010). Then, after noting cases where the T-matrix method might not be the best choice, or even feasible, we review some basic principles of calculating optical forces that can affect the choice of alternative methods.

In general, it is safe to conclude that where calculation of the T-matrix is feasible, the T-matrix method appears to be the ideal method. The T-matrix method is *not* a method of calculating light scattering by a particle, but a formalism in which the *already calculated* scattering properties of the particle can be expressed in the form of the T-matrix. The extended boundary condition method (EBCM) is widely used to calculate the T-matrix, being the original method used by Waterman (1965, 1971). Thus, “T-matrix method” is often used synonymously with EBCM, but the distinction between them should be recognised (Nieminen et al., 2014; Gouesbet, 2010; Gouesbet and Lock, 2015).

In the T-matrix method, we represent the incident and scattered fields in terms of discrete sets of vector-valued basis functions $\psi_n^{(\text{inc})}$ and $\psi_n^{(\text{scat})}$, where n is a mode index labelling the functions, each ψ_n being a solution of the vector Helmholtz equation. Using these bases, we can write the incident field amplitude as

$$\mathbf{E}_0^{(\text{inc})} = \sum_n a_n \psi_n^{(\text{inc})}, \quad (11)$$

where a_n are the *mode amplitudes* (or *expansion coefficients*) of the incident wave, and the scattered wave amplitude as

$$\mathbf{E}_0^{(\text{scat})} = \sum_k p_k \psi_k^{(\text{scat})}, \quad (12)$$

where p_k are the mode amplitudes of the scattered wave. For computational practicality, these sums must be truncated at some finite n_{max} . For a basis set of vector spherical wavefunctions, as usually used in the T-matrix method, the truncation criterion given by Brock is suitable, giving a relative error due to truncation of about 10^{-6} (Nieminen et al., 2011).

With truncation, the mode amplitudes of the incident and scattered waves can be written as column vectors \mathbf{a} and \mathbf{p} , and their relationship can be expressed in matrix form as

$$\mathbf{p} = \mathbf{T}\mathbf{a}, \quad (13)$$

where \mathbf{T} is the *T-matrix*, or transition matrix, or system transfer matrix. This assumes that the electromagnetic properties of the particle are linear and constant (i.e., the particle doesn’t change over time). With this description of scattering, the scattering properties of the particle and the details of the incident field are separated, leading to high efficiency for repeated calculation. Once the T-matrix \mathbf{T}

has been calculated, it can be used repeatedly for calculation under different illumination conditions (as long as the wavelength remains the same). Thus, as the particle moves within the optical trap, the T-matrix \mathbf{T} remains constant, and the incident field, described by \mathbf{a} changes. The changes in \mathbf{a} can be found by using the transformation properties of the basis functions $\psi_n^{(\text{inc})}$ under translation and rotation. It is important to note that the requirement that the particle not change over time means that it is necessary to use a coordinate system in which the particle is fixed. Thus, calculations of the optical force and the torque are performed in the particle rest frame.

Further efficiency results from analytical integration of the momentum flux, using known results for products of integrals of the basis functions over a sphere. This reduces the formulae for optical forces and torques from integrals to sums of products of the mode amplitudes (Nieminen et al., 2014). This avoids the need to calculate the fields over a grid of points in order to perform such integral numerically, and also avoiding numerical error due to the resolution of the computational grid.

However, it is not always feasible to calculate the T-matrix of the particle. The most common methods for calculating the T-matrix of a particle are generalised Lorenz–Mie theory (GLMT), when the particle is a uniform isotropic sphere (but note that GLMTs exist for non-spherical particles as well (Gouesbet and Lock, 2015)) and the extended boundary condition method (EBCM), also known as the null-field method, developed by Waterman (1965, 1971). However, other methods are possible (Mackowski, 2002; Kahnert et al., 2003; Nieminen et al., 2003; Gouesbet, 2010; Mishchenko et al., 2010; Loke et al., 2007, 2009). A comparison of EBCM, point-matching (Nieminen et al., 2003), and the discrete dipole approximation (DDA) (Loke et al., 2009) is given by Qi et al. (2014).

Where it is impractical or impossible to calculate the T-matrix, other methods can be sought. In many ways, the calculation of optical forces and torques is a simple scattering problem. Often, there is a single particle, comparable in size to the wavelength, and sufficiently far from other particles and surfaces so that multiple scattering can be ignored (it should be noted that “multiple scattering” is a rather artificial concept (Mishchenko, 2014), and it is possible to treat scattering by a single object in a multiple scattering formalism (e.g., using DDA) or scattering by a group of objects in a single scattering formalism (Gouesbet and Grehan, 1999)). The incident field is monochromatic and coherent. The complication is that the incident field is not a plane wave, but a focussed beam. This, and the desired outputs being the force and torque rather than the fields, or scattering cross-sections, or scattering patterns, means that existing computational implementations of particular methods might be unsuitable.

There are some general theoretical points that merit discussion, since they can affect the choice of computational method or details of how a method is implemented. In order to calculate the forces, there are two different approaches that we can take. First, we can use conservation of momentum, and find the difference between the incoming momen-

tum flux and the outgoing momentum flux of the light. This difference is the rate at which momentum is transferred to the particle—that is, the force exerted on the particle. Second, we can directly calculate the force using the Lorentz force law (or the Helmholtz force law, or other force law). These two approaches are summarized in figure 1.

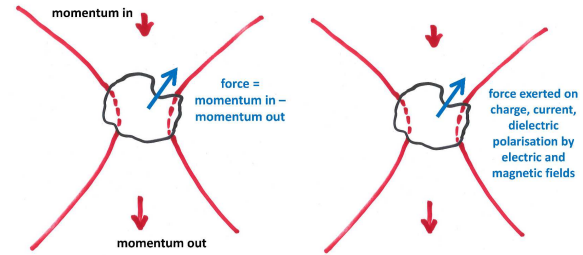


Figure 1: The optical force can be calculated from the momentum flux or by an electromagnetic force law.

At this point, one might be surprised to discover that there are multiple expressions given in the literature for the momentum flux of light, and also multiple electromagnetic force laws. This is the Abraham-Minkowski controversy, where we encounter competing expressions for the momentum density of an electromagnetic field (Pfeifer et al., 2007). With more than one possible expression for the momentum density, how can we choose the correct one, or at least the best one to use?

The key is to note that while there are different expressions for the *electromagnetic* momentum density in material media, the different versions all correspond to identical expressions for the *total* momentum density in the material medium associated with the electromagnetic wave. Where the electromagnetic momenta differ, the difference is matched by opposing differences in what is labelled material momentum or interaction momentum. Since we must calculate the total force, whether or not it is described as purely electromagnetic or the sum of an electromagnetic and a material force, the difference in how the total momentum is divided into electromagnetic and material (and possibly other) components is not fundamental. However, it is convenient to be able to calculate a single quantity rather than multiple quantities that, when added, equal that single quantity. Noting that for cases where the electromagnetic properties of the medium can be described completely with a constant permittivity and permeability, the Minkowski momentum is the total momentum (Pfeifer et al., 2007), this is the simplest choice of momentum density.

With each possible choice of momentum density, there is an associated electromagnetic force law. If we begin by choosing a force law, we can derive an expression for the momentum density and momentum flux of the electromagnetic field. Doing this in reverse, we can begin with an expression for the momentum, and obtain an electromagnetic force law. The most commonly encountered force laws are the Lorentz force law, giving the force acting on charges and currents, and the Helmholtz force law which includes forces acting on induced dipole moments. These connection between these force laws can be seen if we consider the induced dielectric polarisation in a particle. We can represent this either by the dipole moment per unit volume,

or by equivalent charges. For a uniformly polarized sphere, the dipole moment per unit volume is uniform throughout the sphere, but we can replace this by an equivalent surface charge density. In the more general case, we obtain a volume charge density from the variation of the dielectric polarisation in the particle, as shown in figure 2. The Helmholtz force law gives the force acting on the dipole moment per unit volume, and the Lorentz force law the force acting on the equivalent charges. In both cases, the total force is identical.

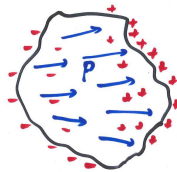


Figure 2: The optical force can be calculated from the momentum flux or by an electromagnetic force law.

If we choose to find the force from conservation of momentum, we need to choose a closed surface over which to integrate the momentum flux. There are three principle choices: a surface conforming to the surface of the trapped particle, a surface of simple geometry close to the particle enclosing it, and a spherical surface in the far field, as shown in figure 3. The latter two of these are often the best choices. If a surface in the far field is chosen, it can be possible to make far-field approximations to simplify calculation of the momentum flux. If a nearby surface of simple geometry is chosen, the same surface can be used for particles of different shapes, simplifying implementation.

If there are multiple particles within the trap, we will usually need to calculate the optical force acting on each particle. This is important, for example, when considering optical binding (Chaumet and Nieto-Vesperinas, 2001; Chvatal et al., 2015). In this case, we cannot find the individual forces by integration of the total field in the far field. We can instead use surface surrounding each individual particle, integration over each of which will yield the force acting on the enclosed particle. In a multiple-particle T-matrix formulation, it is still possible to use the usual single-particle summation formulae (Nieminen et al., 2014) to find the force, if we use incident and scattered field mode amplitudes for each particle individually.

While there are many possible methods, they largely fall into three groups: finite element methods (FEM), finite difference methods, of which the most notable variants are the finite-difference time-domain method (FDTD) and the finite-difference frequency-domain method (FDFD), and approximate methods, notably Rayleigh scattering and geometric optics or ray optics.

In the finite element method (FEM), the computational space is subdivided into finite elements (Volakis et al., 1998). The values relevant to the PDE inside or at the surface of each element are approximated by some known function, perhaps linear or a higher order function (Volakis et al., 1998). The interaction between each element or an element and its surrounding elements is described by a matrix that depends on the particular defini-

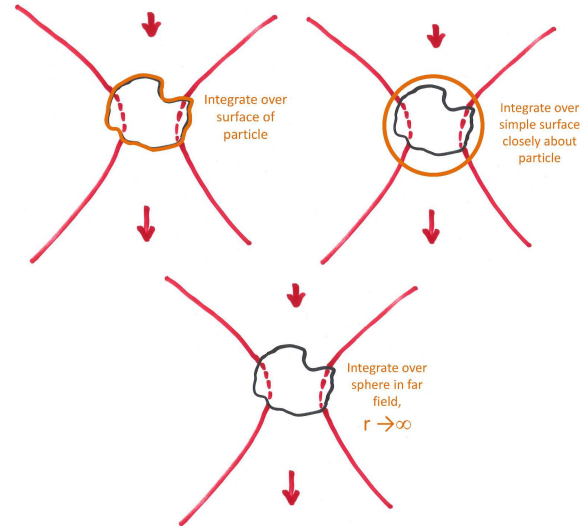


Figure 3: Choices of surface over which to integrate momentum flux. We can choose a surface conforming to the surface of the particle, or a surface of simple geometry enclosing the particle. Alternatively, we can choose a spherical surface in the far field, which can simplify the calculation by allowing us to make far-field approximations.

tion and the chosen division of the computational space. For scattering problems, FEM might be used to refer to a number of methods that involve solving either sparse or dense systems of equations. The most important FEM as far as optical tweezers is concerned is the discrete dipole approximation (DDA). The physical interpretation of DDA involves representing a large scattering particle by multiple smaller interacting dipoles whose polarisability is known (Mishchenko, 2014). The interaction between each dipole is described by a dense matrix; the resulting linear system approximates the scattering by the combined object. Yurkin and Hoekstra (2007) provide a good overview of DDA including recent developments and comparisons to other methods. Unlike other FEM, DDA doesn't require the space surrounding the scatter to be discretised, unless the surrounding space is inhomogeneous or contains other objects. DDA is more suitable for smaller isolated particles and particles with smaller (relative) refractive indexes due to the requirement to solve a dense linear system.

The finite-difference time-domain (FDTD) method refers to a method described by Yee (1966) for solving systems of coupled partial differential equations. Although it was originally formulated for solving the Maxwell equations, FDTD can also be applied to other systems of differential equations. The original formulation of FDTD for the Maxwell equations involved calculating the electric and magnetic fields at locations on a structured grid spanning the computational space. Spatial derivatives in the Maxwell equations are calculated using second order finite difference approximations involving the adjacent locations on the structured grid. The fields are advanced through time using a leapfrog scheme with second order accuracy, where the electric and magnetic fields are updated at alternate half integer time steps. Since Yee's original method, there have been numerous improvements and specialisations such as unconditionally stable methods or single step methods (Inan and Marshall, 2011; Raedt et al.,

2003). One disadvantage of the FDTD method is difficulty in representing objects with smooth surfaces using a structured Cartesian grid; when the surface doesn't conform to the Cartesian grid, this introduces staircasing error (Inan and Marshall, 2011). The simplest approach is to increase the grid resolution. However, this results in a major increase in the computational requirements. Other alternatives include using non-Cartesian grids such as spherical or circular grids, sub-gridding certain regions or incorporating a local distortion near curved object boundaries (Hastings et al., 2001). Use of non-Cartesian grids requires calculation of the Jacobian and correcting the FDTD update equations appropriately, special attention should also be given to discontinuities in the mesh.

The finite-difference frequency-domain (FDFD) method is very similar to FDTD except it assumes time harmonic solutions for the incident and scattered fields (Loke et al., 2007). FDFD is very similar to FEM where only interactions between adjacent elements are considered. This results in a linear system describing the scatter. Unlike FDTD, FDFD performs the scattering calculation for only a particular frequency, while FDTD is able to calculate the scattering of multiple frequencies simultaneously.

The choice to use a particular computational method to model optical tweezers greatly depends on the regime the problem falls into. For very large and very small particles the ray optics and Rayleigh approximations are able to model particles with reasonable accuracy. DDA approaches the Rayleigh limit for small particles but is able to simulate larger particles with fairly high accuracy but scales relatively poorly with memory and time. The FDTD and FDFD methods are able to simulate an extended range of particles but rely on being able to discretise the computational space to describe fine details of the scatterer or rapidly changing fields. FDFD assumes a particular form for the wave solutions, but is only able to simulate a single frequency; in comparison, FDTD can easily deal with illumination such as short pulses, and can include non-linear effects including frequency doubling, frequency mixing, etc. A summary of these comparisons is presented graphically in figure 4. The performance and capabilities of the different methods depend on the type of problem being solved, so this comparison should be treated as a qualitative guide, rather than an exact quantitative comparison. This comparison is based on our own experience with these methods.

4. Viscous drag

Viscous drag is a key factor in the dynamics of a particle in an optical trap. It determines the speed at which the optical forces and torques will move or rotate the particle, and it also affects Brownian motion. For simulation of optical tweezers, we wish to obtain the translational viscous drag tensor for the particle (and the rotational drag tensor, if we need to include rotation in the simulation). For the case of a spherical particle, this is straightforward, since there is a simple analytical solution: Stokes drag on a sphere. This gives

$$\mathbf{D} = 6\pi\eta a\mathbf{I}, \quad (14)$$

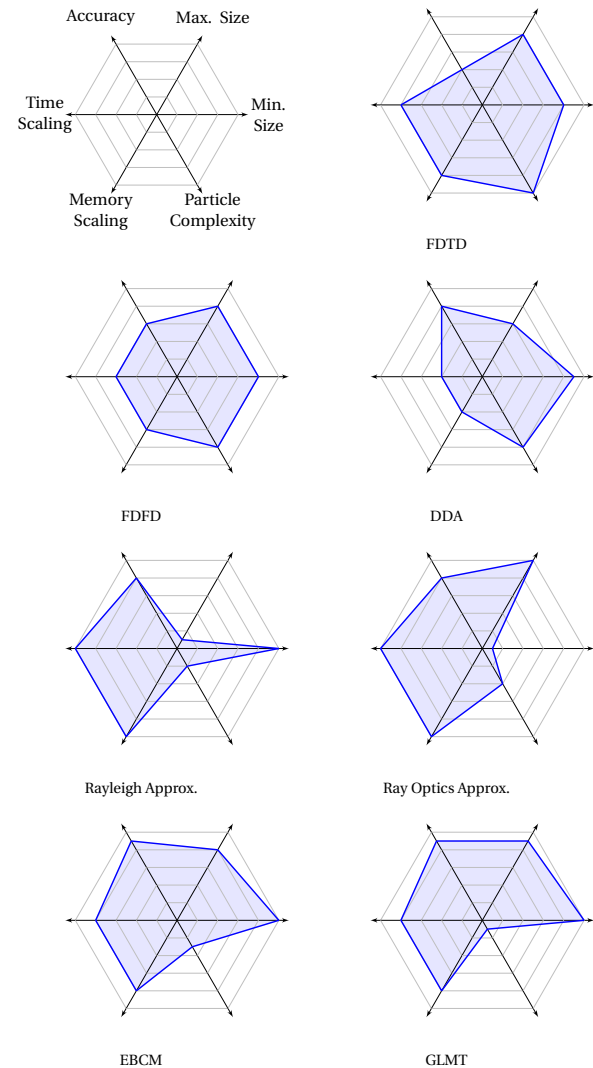


Figure 4: Comparison of different computational methods for simulating optical tweezers. Further from the centre is better; e.g., the Rayleigh approximation, GLMT and EBCM are the best of these methods for calculation forces on very small particles. The particle complexity includes both the particle geometry and composition (inhomogeneity, anisotropy, non-linearity). The accuracy and computational requirements depend on the type of problem being solved, so this comparison should be treated as a qualitative guide, rather than an exact quantitative comparison.

where \mathbf{I} is the identity tensor. If the rotational drag tensor is required, this is equal to

$$\mathbf{D}_{\text{rot}} = 8\pi\eta a^3 \mathbf{I}. \quad (15)$$

For cylinders, convenient formulae are given by de la Torre and Bloomfield (1981). For more general cases, it can be necessary to resort to solving the fluid flow and calculating the drag tensors. At low Reynolds numbers, the fluid flow is described by the Stokes equation:

$$\eta \nabla^2 \mathbf{v} = \nabla p, \quad (16)$$

where \mathbf{v} is the velocity field of the fluid flow, and p is the pressure field. The two most promising approaches appear to be using the general solution in spherical coordinates (Lamb, 1924; Pak and Lauga, 2014) and direct finite-difference solution.

4.1. Wall effects

It should also be noted that nearby surfaces affect the viscous drag on a particle. In general, this is a difficult problem (Happel and Brenner, 1991). However, the simple case of a sphere near a plane wall has a known solution. The approximate solution by Faxén (1922) is often used. However, it is only accurate when the particle is a large distance away from the wall, and fails when the distance between the wall and the closest part of the particle is less than 1 particle radius. That is, it cannot be used when it is most needed. The exact solution presents serious difficulties in calculation. Fortunately, a simple and very accurate approximation formula is available (Chaoui and Feuillebois, 2003).

5. A recipe for simulation, part 2: Brownian motion

Brownian motion in a viscous fluid, in the absence of other forces, can be easily modelled. The probability distributions for displacements of a spherical particle in each of the x , y , and z directions over a time interval Δt are normal (Gaussian), with variance equal to $2D\Delta t$, where

$$D = \frac{k_B T}{6\pi\eta a} \quad (17)$$

is the diffusion coefficient, and k_B is Boltzmann’s constant, T is the absolute temperature, η is the (dynamic) viscosity, and a is the radius of particle. Thus, it is straightforward to simulate Brownian motion using a Monte Carlo method. To calculate a displacement over Δt , we can generate 3 normally distributed random numbers, R_x , R_y , and R_z with variance equal to 1, giving us

$$\Delta x = (2D\Delta t)^{1/2} R_x \quad (18)$$

for the displacement in the x -direction, and similar results in the y and z directions. This can then be repeated for subsequent time steps, with new random numbers R_x , R_y , and R_z generated for each time step.

Notably, classical Brownian motion of this type is self-similar across all time scales, i.e., fractal (Einstein, 1956; Nelson, 1967), and consequently, the accuracy of a Monte Carlo simulation like this is independent of the choice of step size Δt . Therefore, if we aim to simulate a series of

measurements of particle position, it is sufficient to calculate the particle position at only the times at which the position is measured, and Δt is the time interval between the measurements. There is no need to calculate the position for intermediate times.

However, in the presence of other forces, this changes. It becomes necessary for the distance the particle moves in a single time step to be small enough so that the other forces do not change too much. Since the optical force can change greatly over half a wavelength, the distance must be a small fraction of the wavelength. Noting that a particle of radius $1\ \mu\text{m}$ will move, on average, a distance of $1\ \mu\text{m}$ in 2.1 s due to Brownian motion in water at 300 K, and the distance scales with the square root of Δt , we would need a time step of approximately 10^{-4} s if we want the distance moved to be less than 1% of the wavelength.

We can investigate the effect of our choice of time step quantitatively. We can generate a series of discrete Brownian steps for a time step Δt_0 , and calculate the motion of the particle. Then, we can double the time step, and sum successive pairs of Brownian steps, to obtain half the number of steps, each twice as long in time. This can be repeated, allowing us to investigate the convergence of the calculation with decreasing time step. The displacement over the time step due to Brownian motion can be used to find an average velocity due to Brownian motion over the time step; this can be expressed as an average force over the time step and included in a predictor–corrector method such as Runge–Kutta. An example is shown in figure 5 for a particle of radius $1\ \mu\text{m}$, comparing the convergence of trajectories as the time step is reduced. The comparison includes both Euler’s method and a fixed-step 4th-order Runge–Kutta method. The results indicate that a time step of 10^{-4} s (for a distance less than 1% of the wavelength) gives a reasonably small error. If higher accuracy is desired, a shorter time step can be chosen. Due to the square root dependence of the distance, the scaling is relatively poor.

We recommend that a similar analysis of convergence be performed, especially if simulations are sufficiently lengthy so that a just-small-enough for acceptable error time-step should be chosen.

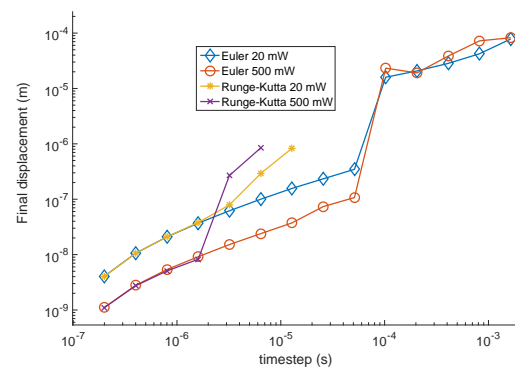


Figure 5: Convergence of final position of particle undergoing Brownian motion in an optical trap as a function of time step.

For very short time steps, the Stokes drag formula can be inappropriate (Franosch et al., 2011; Kheifets et al., 2014),

and for very short time steps, the transition to ballistic motion becomes apparent (Huang et al., 2011). As long as the time step is not too short, this will not present any difficulty. If simulations of a particle trapped in gas are being performed, then the transition between ballistic and continuous regimes is important (Li et al., 2010) at larger time steps.

5.1. Nonspherical particles

If the particle is nonspherical, the translation and rotational drag tensors will be different in different directions, and the variance of the Brownian motion will be different in different directions.

It is simplest to calculate the random Brownian steps in the rest frame of the particle, and then transform the motion to the stationary frame.

The question of suitable time steps was left open earlier. From the discussion of Brownian motion above, we see that Brownian motion can be the main factor limiting our choice of time step. However, it is wise to check that the optical force will not move the particle too far during the time step. A maximum time step based on the optical force can be found, and another based on the Brownian motion. The smaller of the two can then be used as the actual time step for the computation. If Brownian motion can be neglected, then it can be convenient to use an adaptive step size solver for initial value problems. If we wish to calculate simulated measured at specific times, we can choose time steps so that these specific times match times at which we calculate the position of the particle in the trap. Alternatively, it may be possible to interpolate between the calculations.

6. Open questions

A number of open questions and unsolved problems in simulation of optical tweezers remain. We present a selection of them here, in the spirit of presenting useful and interesting challenges to those who wish to tackle them. Interesting work has been performed on some of these topics, giving a hint of many interesting results yet to be uncovered.

- **Optical force on complex particles.** While optical forces and torques exerted on a wide range of particles can be readily calculated, those on large and complex particles remain challenging.
- **Nonlinear particles.** Particles with non-linear electromagnetic properties have the potential for many interesting behaviours in optical traps (Pobre and Saloma, 1997, 2006; Devi and De, 2016).
- **Deformable particles.** These present a double challenge. First, it is necessary to calculate not just the optical and viscous forces acting on the particle, but also the stresses and consequent deformation of the particle. Second, the deformation results in change in the optical force. The deformable particles of most interest are red blood cells (Li et al., 2005; Dao et al., 2003; Rancourt-Grenier et al., 2010) and other cells

(Guck et al., 2005), but simpler objects such as vesicles, which are sometimes used as simple analogs of cells, are also of interest (Noguchi and Takasu, 2002).

- **Wall effects on viscous drag on non-spherical particles.**

The movement of non-spherical particles near surfaces is important in many biological systems. One interesting example is the motion of sperm, which dramatically change in their swimming behaviour near surfaces. (Elgeti et al., 2010; Nosrati et al., 2015). Optical tweezers offers an opportunity to explore this behaviour, either by trapping sperm and measuring swimming forces (as done for free-swimming sperm by Nascimento et al. (2008)) or by trapping and moving analogs near surfaces. Simulations would be very helpful for identifying changes in motion that result from changed behaviour of sperm near surfaces; such simulations would need to account for wall effects on the motion.

- **Interaction between trapped particles and complex biological environments.**

The work on deformation of red blood cells noted above can be considered a special case of this. More generally, a trapped particle can interact with membranes, macromolecules, cells, complex fluids, etc. Modelling its interaction with such an environment can be challenging. Where the behaviour of living cells needs to be included (e.g., swimming behaviour of bacteria or sperm, ingestion of the trapped particle by a macrophage, etc.), realistic models of the behaviour are required. This is a very complex problem that remains largely untouched.

- **Heating and thermal effects, including convective flow.**

While heating is often ignored in optical trapping simulations—wavelengths and beam powers are often chosen to be such that absorption and consequent heating is minimal, to avoid damage to live biological specimens—there can be significant heating when absorbing particles are trapped. Heating introduces a wide range of effects, from changes in the viscosity of the surrounding fluid due to increased temperature, convection currents, and effects such as thermophoresis (Flores-Flores et al., 2015). If there are liquid-liquid or liquid-gas interfaces present, the dependence of surface tension on temperature can produce strong flows due to Marangoni convection (Miniewicz et al., 2016). In general, the temperature distribution drives the convective flows, and the convective flows can alter the temperature distribution, and also the position of the particle within the trap (thus altering the absorption of light and the temperature distribution). This coupling makes the solution of the problem difficult; an iterative method might be required. The time scales involved can be investigated—if conduction dominates energy transport, then it may be possible to ignore the effect of convection on the tempera-

ture distribution, and the problem, while still challenging, is greatly simplified.

Acknowledgments

This research was supported under Australian Research Council's Discovery Projects funding scheme (project number DP140100753).

References

- Aguilar-Ibañez, C., Suarez-Castanon, M. S., Rosas-Soriano, L. I., 2011. A simple control scheme for the manipulation of a particle by means of optical tweezers. *International Journal of Robust and Nonlinear Control* 21 (3), 328–337.
- Artusio-Glimpse, A. B., Peterson, T. J., Swartzlander, G. A., 2013. Refractive optical wing oscillators with one reflective surface. *Optics Letters* 38 (6), 935–937.
- Artusio-Glimpse, A. B., Schuster, D. G., Gomes, M. W., Swartzlander, G. A., 2014. Rocking motion of an optical wing: theory. *Applied Optics* 53 (31), 11–19.
- Banerjee, A., Balijepalli, A., Gupta, S. K., LeBrun, T. W., 2009. Generating simplified trapping probability models from simulation of optical tweezers system. *J. Comput. Inf. Sci. Eng.* 9 (2), 021003.
- Banerjee, A. G., Chowdhury, S., Losert, W., Gupta, S. K., 2012. Real-time path planning for coordinated transport of multiple particles using optical tweezers. *IEEE Transactions on Automation Science and Engineering* 9, 669–678.
- Bayouh, S., Nieminen, T. A., Heckenberg, N. R., Rubinsztein-Dunlop, H., 2003. Orientation of biological cells using plane polarised Gaussian beam optical tweezers. *Journal of Modern Optics* 50 (10), 1581–1590.
- Brzobohatý, O., Arzola, A. V., Šiler, M., Chvátal, L., Ják, P., Simpson, S., Zemánek, P., 2015a. Complex rotational dynamics of multiple spheroidal particles in a circularly polarized, dual beam trap. *Opt. Express* 23 (6), 7273–7287.
- Brzobohatý, O., Šiler, M., Trojek, J., Chvátal, L., Karásek, V., Zemánek, P., 2015b. Non-spherical gold nanoparticles trapped in optical tweezers: shape matters. *Opt. Express* 23 (7), 8179–8189.
- Bui, A. A. M., Stilgoe, A. B., Khatibzadeh, N., Nieminen, T. A., Berns, M. W., Rubinsztein-Dunlop, H., 2015. Escape forces and trajectories in optical tweezers and their effect on calibration. *Opt. Express* 23 (19), 24317–24330.
- Bui, A. A. M., Stilgoe, A. B., Nieminen, T. A., Rubinsztein-Dunlop, H., 2013. Calibration of nonspherical particles in optical tweezers using only position measurement. *Optics Letters* 38 (8), 1244–1246.
- Cao, Y., Stilgoe, A. B., Chen, L., Nieminen, T. A., Rubinsztein-Dunlop, H., 2012. Equilibrium orientations and positions of non-spherical particles in optical traps. *Optics Express* 20, 12987–12996.
- Cao, Y., Zhu, T., Lv, H., Ding, W., 2016. Spin-controlled orbital motion in tightly focused high-order laguerre-gaussian beams. *Opt. Express* 24 (4), 3377–3384.
- Chaoui, M., Feuillebois, F., 2003. Creeping flow around a sphere in a shear flow close to a wall. *Q. J. Mech. Appl. Math.* 56 (3), 381–410.
- Chaumet, P. C., Nieto-Vesperinas, M., 2001. Optical binding of particles with or without the presence of a flat dielectric surface. *Physical Review B* 64, 035422.
- Chvátal, L., Brzobohatý, O., Zemanek, P., 2015. Binding of a pair of Au nanoparticles in a wide Gaussian standing wave. *Optical Review* 22, 157–161.
- Czerwinski, F., Richardson, A. C., Oddershede, L. B., 2009. Quantifying noise in optical tweezers by Allan variance. *Opt. Express* 17 (15), 13255–13269.
- Dao, M., Lim, C., Suresh, S., 2003. Mechanics of the human red blood cell deformed by optical tweezers. *Journal of the Mechanics and Physics of Solids* 51, 2259–2280.
- de la Torre, J. G. G., Bloomfield, V. A., 1981. Hydrodynamic properties of complex, rigid, biological macromolecules: theory and applications. *Q. Rev. Biophys.* 14 (1), 81–139.
- Deng, Y., Bechhoefer, J., Forde, N. R., 2007. Brownian motion in a modulated optical trap. *Journal of Optics A* 9 (8), S256.
- Devi, A., De, A. K., 2016. Theoretical investigation on nonlinear optical effects in laser trapping of dielectric nanoparticles with ultrafast pulsed excitation. *Optics Express* 24 (19), 21485.
- Einstein, A., 1956. *Investigations on the theory of the Brownian movement*. Dover, New York.
- Elgeti, J., Kaupp, U. B., Gompper, G., 2010. Hydrodynamics of sperm cells near surfaces. *Biophys J.* 99 (4), 1018–1026.
- Faxén, H., 1922. Der Widerstand gegen die Bewegung einer starren Kugel in einer zähen Flüssigkeit, die zwischen zwei parallelen ebenen Wänden eingeschlossen ist. *Annalen der Physik* 373 (10), 89–119.
- Ferraro-Gideon, J., Sheykhan, R., Zhu, Q., Duquette, M. L., Berns, M. W., Forer, A., 2014. Measurements of forces produced by the mitotic spindle using optical tweezers. *Mol. Biol. Cell* 24, 1375–1386.
- Fischer, M., Berg-Sørensen, K., 2007. Calibration of trapping force and response function of optical tweezers in viscoelastic media. *Journal of Optics A: Pure and Applied Optics* 9, S239–S250.
- Flores-Flores, E., Torres-Hurtado, S. A., Páez, R., Ruiz, U., Beltrán-Pérez, G., Neale, S. L., Ramirez-San-Juan, J. C., Ramos-García, R., 2015. Trapping and manipulation of microparticles using laser-induced convection currents and photophoresis. *Biomed Opt Express* 6 (10), 4079–4087.
- Franosch, T., Grimm, M., Belushkin, M., Mor, F. M., Foffi, G., Forró, L., Jeney, S., 2011. Resonances arising from hydrodynamic memory in Brownian motion. *Nature* 478, 85–88.
- Gong, Z., Chen, H., Xu, S., Li, Y., Lou, L., 2006. Monte-Carlo simulation of optical trap stiffness measurement. *Optics Communications* 263 (2), 229–234.
- Gouesbet, G., 2010. T-matrix formulation and generalized Lorenz-Mie theories in spherical coordinates. *Optics Communications* 283, 517–521.
- Gouesbet, G., Grehan, G., 1999. Generalized Lorenz-Mie theory for assemblies of spheres and aggregates. *Journal of Optics A: Pure and Applied Optics* 1, 706–712.
- Gouesbet, G., Lock, J. A., 2015. On the electromagnetic scattering of arbitrary shaped beams by arbitrary shaped particles: A review. *Journal of Quantitative Spectroscopy and Radiative Transfer* 162, 31–49.
- Guck, J., Schinkinger, S., Lincoln, B., Wottawah, F., Ebert, S., Romeyke, M., Lenz, D., Erickson, H. M., Ananthakrishnan, R., Mitchell, D., Kas, J., Ulvick, S., Bilby, C., 2005. Optical deformability as an inherent cell marker for testing malignant transformation and metastatic competence. *Biophysical Journal* 88 (5), 3689–3698.
- Haghshenas-Jaryani, M., Black, B., Ghaffari, S., Drake, J., Bowling, A., Mohanty, S., 2014. Dynamics of microscopic objects in optical tweezers: experimental determination of underdamped regime and numerical simulation using multiscale analysis. *Nonlinear Dynamics* 76, 1013–1030.
- Happel, J., Brenner, H., 1991. *Low Reynolds Number Hydrodynamics*. Kluwer, Dordrecht.
- Hastings, F. D., Schneider, J. B., Broschat, S. L., Thorsos, E. I., 2001. An FDTD method for analysis of scattering from rough fluid-fluid interfaces. *IEEE Journal of Oceanic Engineering* 26 (1), 94–101.
- Huang, R., Chavez, I., Taute, K. M., Lukić, B., Jeney, S., Raizen, M. G., Florin, E.-L., 2011. Direct observation of the full transition from ballistic to diffusive Brownian motion in a liquid. *Nature Physics* 7, 576–580.
- Inan, U. S., Marshall, R. A., 2011. *Numerical electromagnetics: the FDTD method*. Cambridge University Press, Cambridge.
- Jones, P. H., Maragò, O. M., Volpe, G., 2015. *Optical Tweezers: Principles and Applications*. Cambridge University Press, Cambridge.
- Kahnert, F. M., 2003. Numerical methods in electromagnetic scattering theory. *Journal of Quantitative Spectroscopy and Radiative Transfer* 79–80, 775–824.
- Kahnert, F. M., Stamnes, J. J., Stamnes, K., 2003. Surface-integral formulation for electromagnetic scattering in spheroidal coordinates. *Journal of Quantitative Spectroscopy and Radiative Transfer* 77, 61–78.
- Khatibzadeh, N., Stilgoe, A. B., Bui, A. A. M., Rocha, Y., Cruz, G. M., Loke, V., Shi, L. Z., Nieminen, T. A., Rubinsztein-Dunlop, H., Berns, M. W., 2014. Determination of motility forces on isolated chromosomes with laser tweezers. *Scientific Reports* 4, 6866.
- Kheifets, S., Simha, A., Melin, K., Li, T., Raizen, M. G., 2014. Observation of Brownian motion in liquids at short times: Instantaneous velocity and memory loss. *Science* 343, 1493–1496.
- Lamb, H., 1924. *Hydrodynamics*, 5th Edition. Cambridge University Press, Cambridge.
- Li, J., Dao, M., Lim, C., Suresh, S., 2005. Spectrin-level modeling of the cytoskeleton and optical tweezers stretching of the erythrocyte. *Biophysical Journal* 88, 3707–3719.
- Li, T., Kheifets, S., Medellin, D., Raizen, M. G., 2010. Measurement of the instantaneous velocity of a Brownian particle. *Science* 328, 1673–1675.

- Li, X., Cheah, C. C., Hu, S., Sun, D., 2013. Dynamic trapping and manipulation of biological cells with optical tweezers. *Automatica* 49 (6), 1614–1625.
- Loke, V. L. Y., Asavei, T., Stilgoe, A. B., Nieminen, T. A., Rubinsztein-Dunlop, H., 2014. Driving corrugated donut rotors with laguerre-gauss beams. *Opt. Express* 22 (16), 19692–19706.
- Loke, V. L. Y., Nieminen, T. A., Heckenberg, N. R., Rubinsztein-Dunlop, H., 2009. *T*-matrix calculation via discrete dipole approximation, point matching and exploiting symmetry. *Journal of Quantitative Spectroscopy and Radiative Transfer* 110, 1460–1471.
- Loke, V. L. Y., Nieminen, T. A., Parkin, S. J., Heckenberg, N. R., Rubinsztein-Dunlop, H., 2007. FDFD/*T*-matrix hybrid method. *Journal of Quantitative Spectroscopy and Radiative Transfer* 106, 274–284.
- Loudet, J.-C., Mihiretie, B. M., Pouligny, B., 2014. Optically driven oscillations of ellipsoidal particles. Part II: Ray-optics calculations. *The European Physical Journal E* 37, 125.
- Mackowski, D. W., May 2002. Discrete dipole moment method for calculation of the *t* matrix for nonspherical particles. *Journal of the Optical Society of America A* 19 (5), 881–893.
- Mihiretie, B. M., Snabre, P., Loudet, J. C., Pouligny, B., 2014. Optically driven oscillations of ellipsoidal particles. Part I: experimental observations. *The European Physical Journal E* 37, 124.
- Miniewicz, A., Bartkiewicz, S., Orlikowska, H., Dradrach, K., 2016. Marangoni effect visualized in two-dimensions Optical tweezers for gas bubbles. *Scientific Reports* 6, 34787.
- Mishchenko, M. I., 2014. *Electromagnetic Scattering by Particles and Particle Groups*. Cambridge University Press, Cambridge.
- Mishchenko, M. I., Travis, L. D., Mackowski, D. W., 2010. *T*-matrix method and its applications to electromagnetic scattering by particles: A current perspective. *Journal of Quantitative Spectroscopy and Radiative Transfer* 111, 1700–1703.
- Moffatt, H. K., 1977. Six lectures on general fluid dynamics and two on hydromagnetic dynamo theory. In: Balian, R., Peube, J.-L. (Eds.), *Fluid dynamics*. Gordon and Breach, London, pp. 149–233.
- Nascimento, J. M., Shi, L. Z., Chandsawangbhuwana, C., Tam, J., Durrant, B., Botvinick, E. L., Berns, M. W., 2008. Use of laser tweezers to analyze sperm motility and mitochondrial membrane potential. *J Biomed Opt.* 13, 014002.
- Nelson, E., 1967. *Dynamical Theories of Brownian Motion*. Princeton University Press.
- Nieminen, T. A., du Preez-Wilkinson, N., Stilgoe, A. B., Loke, V. L. Y., Bui, A. A. M., Rubinsztein-Dunlop, H., 2014. Optical tweezers: Theory and modelling. *Journal of Quantitative Spectroscopy and Radiative Transfer* 146, 59–80.
- Nieminen, T. A., Loke, V. L. Y., Stilgoe, A. B., Heckenberg, N. R., Rubinsztein-Dunlop, H., 2011. *T*-matrix method for modelling optical tweezers. *Journal of Modern Optics*, 528–544.
- Nieminen, T. A., Rubinsztein-Dunlop, H., Heckenberg, N. R., 2001. Calculation and optical measurement of laser trapping forces on non-spherical particles. *Journal of Quantitative Spectroscopy and Radiative Transfer* 70, 627–637.
- Nieminen, T. A., Rubinsztein-Dunlop, H., Heckenberg, N. R., 2003. Calculation of the *t*-matrix: general considerations and application of the point-matching method. *Journal of Quantitative Spectroscopy and Radiative Transfer* 79-80, 1019–1029.
- Noguchi, H., Takasu, M., 2002. Structural changes of pulled vesicles: A Brownian dynamics simulation. *Phys. Rev. E* 65, 051907.
- Nosrati, R., Driouchi, A., Yip, C. M., Sinton, D., 2015. Two-dimensional slither swimming of sperm within a micrometre of a surface. *Nature Communications* 6, 8703.
- Pak, O. S., Lauga, E., 2014. Generalized squirming motion of a sphere. *Journal of Engineering Mathematics* 88 (1), 1.
- Perkins, T. T., Malley, C. V., Dubson, M., Perkins, K. K., 2010. An interactive optical tweezers simulation for science education. *Proc. SPIE* 7762, 776215.
- Pesce, G., Volpe, G., Chiara De Luca, A., Rusciano, G., Volpe, G., 2009. Quantitative assessment of non-conservative radiation forces in an optical trap. *EPL* 86, 38002.
- Pfeifer, R. N. C., Nieminen, T. A., Heckenberg, N. R., Rubinsztein-Dunlop, H., 2007. Momentum of an electromagnetic wave in dielectric media. *Reviews of Modern Physics* 79 (4), 1197–1216.
- Pobre, R., Saloma, C., 1997. Single Gaussian beam interaction with a Kerr microsphere: characteristics of the radiation force. *Applied Optics* 36, 3515–3520.
- Pobre, R., Saloma, C., 2006. Radiation force exerted on nanometer size non-resonant Kerr particle by a tightly focused Gaussian beam. *Optics Communications* 267, 295–304.
- Purcell, E. M., Jan. 1977. Life at low Reynolds number. *American Journal of Physics* 45 (1), 3–11.
- Qi, X., Nieminen, T. A., Stilgoe, A. B., Loke, V. L. Y., Rubinsztein-Dunlop, H., 2014. Comparison of *T*-matrix calculation methods for scattering by cylinders in optical tweezers. *Opt. Lett.* 39, 4827–4830.
- Raedt, H. D., Michielsens, K., Kole, J. S., Figge, M. T., 2003. Solving the Maxwell equations by the Chebyshev method: a one-step finite-difference time-domain algorithm. *IEEE Transactions on Antennas and Propagation* 51 (11), 3155–3160.
- Rancourt-Grenier, S., Wei, M.-T., Bai, J.-J., Chiou, A., Bareil, P. P., Duval, P.-L., Sheng, Y., 2010. Dynamic deformation of red blood cell in dual-trap optical tweezers. *Opt. Express* 18 (10), 10462–10472.
- Ren, Y., Wu, J., Zhong, M., Li, Y., 2010. Monte-Carlo simulation of effective stiffness of time-sharing optical tweezers. *Chin. Opt. Lett.* 8 (2), 170–172.
- Simpson, S. H., Hanna, S., 2010a. Holographic optical trapping of micro-rods and nanowires. *J. Opt. Soc. Am. A* 27 (6), 1255–1264.
- Simpson, S. H., Hanna, S., 2010b. Orbital motion of optically trapped particles in Laguerre–Gaussian beams. *J. Opt. Soc. Am. A* 27 (9), 2061–2071.
- Simpson, S. H., Hanna, S., Peterson, T. J., Swartzlander, G. A., 2012. Optical lift from dielectric semicylinders. *Optics Letters* 37 (19), 4038–4040.
- Stilgoe, A. B., Heckenberg, N. R., Nieminen, T. A., Rubinsztein-Dunlop, H., 2011. Phase-transition-like properties of double-beam optical tweezers. *Physical Review Letters* 107, 248101.
- Taylor, M. A., Waleed, M., Stilgoe, A. B., Rubinsztein-Dunlop, H., Bowen, W. P., 2015. Enhanced optical trapping via structured scattering. *Nature Photonics* 9, 669–673.
- Trojek, J., Chvátal, L., Zemánek, P., 2012. Optical alignment and confinement of an ellipsoidal nanorod in optical tweezers: a theoretical study. *J. Opt. Soc. Am. A* 29 (7), 1224–1236.
- Volakis, J. L., Chatterjee, A., Kempel, L. C., 1998. *Finite element method for electromagnetics: antennas, microwave circuits, and scattering applications*. IEEE Press, New York.
- Volpe, G., Kurz, L., Callegari, A., Volpe, G., Gigan, S., 2014. Speckle optical tweezers: micromanipulation with random light fields. *Opt. Express* 22 (15), 18159–18167.
- Volpe, G., Petrov, D., 2006. Torque detection using Brownian fluctuations. *Phys. Rev. Lett.* 97, 210603.
- Volpe, G., Volpe, G., 2013. Simulation of a Brownian particle in an optical trap. *American Journal of Physics* 81, 224–230.
- Volpe, G., Volpe, G., Petrov, D., 2007. Brownian motion in a nonhomogeneous force field and photonic force microscope. *Phys. Rev. E* 76, 061118.
- Waterman, P. C., Aug. 1965. Matrix formulation of electromagnetic scattering. *Proceedings of the IEEE* 53 (8), 805–812.
- Waterman, P. C., 1971. Symmetry, unitarity, and geometry in electromagnetic scattering. *Physical Review D* 3, 825–839.
- Wu, P., Huang, R., Tischer, C., Jonas, A., Florin, E.-L., 2009. Direct measurement of the nonconservative force field generated by optical tweezers. *Phys. Rev. Lett.* 103, 108101.
- Xu, S.-H., Li, Y.-M., Lou, L.-R., Sun, Z.-W., 2005. Computer simulation of the collision frequency of two particles in optical tweezers. *Chinese Physics* 14 (2), 382–385.
- Yee, K. S., May 1966. Numerical solution of initial boundary value problems involving Maxwell's equations in isotropic media. *IEEE Transactions on Antennas and Propagation* 14 (3), 302–307.
- Yurkin, M. A., Hoekstra, A. G., 2007. The discrete dipole approximation: An overview and recent developments. *Journal of Quantitative Spectroscopy and Radiative Transfer* 106, 558–589.